Three-dimensional structural dynamics of myosin V by single-molecule fluorescence polarization

Joseph N. Forkey*, Margot E. Quinlan*, M. Alexander Shaw*, John E. T. Corrie† & Yale E. Goldman*

** Pennsylvania Muscle Institute, University of Pennsylvania, Philadelphia, Pennsylvania 19104-6083, USA*
† National Institute for Medical Research, Mill Hill, London NW7 1AA, UK

The structural change that generates force and motion in actomyosin motility has been proposed to be tilting of the myosin light chain domain, which serves as a lever arm. Several experimental approaches have provided support for the lever arm hypothesis; however, the extent and timing of tilting motions are not well defined in the motor protein complex of functioning actomyosin. Here we report three-dimensional measurements of the structural dynamics of the light chain domain of brain myosin V using a single-molecule fluorescence polarization technique that determines the orientation of individual protein domains with 20–40-ms time resolution. Single fluorescent calmodulin light chains tilted back and forth between two well-defined angles as the myosin molecule processively translocated along actin. The results provide evidence for lever arm rotation of the calmodulin-binding domain in myosin V, and support a 'hand-over-hand' mechanism for the translocation of double-headed myosin V molecules along actin filaments. The technique is applicable to the study of real-time structural changes in other biological systems.

Force and translocation in actomyosin systems are thought to be generated by motions in which the myosin light chain domain (LCD) acts as a mechanical lever arm. In the lever arm hypothesis, the amino-terminal motor domain of myosin binds stereospecifically to actin while the LCD rotates relative to the motor domain[1,2]. The motor domain and LCD can occupy a number of relative orientations[3,4], and LCD rotations accompany translocation and force generation in muscle fibres[5,6]. Despite extensive work, however, time-resolved angle changes of the LCD with appropriate magnitude to explain observed stepping distances and velocities have not yet been demonstrated clearly in an active system.

X-ray crystallography and cryo-electron microscopy provide high spatial resolution but they cannot measure changes in a functioning sample over time. On the other hand, techniques such as spectroscopy and low-angle X-ray diffraction of bulk samples, such as muscle fibres, have provided good temporal resolution, but are difficult to quantify and interpret structurally because averaging among unsynchronized populations of molecules reduces the signal changes. To circumvent these difficulties, we have developed a single-molecule fluorescence polarization technique, which is able to determine the orientation of individual protein domains to a time resolution of 20–40 ms. This method detects the mean three-dimensional orientation as well as the amplitude of wobble occupying the timescale $\gg$4 ns to $\ll$10 ms. Here we report its use to observe, in real time, large angle changes in the LCD of individual myosin V molecules, with magnitude and dynamics consistent with the lever arm hypothesis.

We used myosin V for this study because its specific enzymatic and mechanical features[7–10] confer advantages for single-molecule fluorescence polarization measurements. Individual double-headed myosin V molecules move along actin with high processivity[11,12], undergoing many biochemical cycles and multiple 36–37-nm mechanical steps for each encounter with an actin filament. A myosin V molecule frequently moves along an actin filament for several seconds, allowing the determination of its velocity followed by measurement of orientation changes during several catalytic cycles. The most widely held hypothesis that explains myosin V processivity is the so-called 'hand-over-hand' model, which predicts that each head spends most of its ATPase cycle attached to the actin filament, either leading or trailing its partner head. Stepping events are thought to occur through detachment of the trailing head, rapid forward motion of this head by about 74 nm, and reattachment as the new leading head, while the other head remains attached[8,11,13–15]. The translation of the detached head from trailing to leading position is thought to be generated mainly by tilting of the LCD of the attached head. On the basis of this model, we expected to observe two discrete orientations of the myosin V LCD with similar lifetimes, corresponding to the two head positions.

Time-resolved single-molecule fluorescence polarization

Calmodulin (CaM) was labelled with bisiodoacetamidorhodamine[16,17] at a known orientation (see Supplementary Information) relative to the molecular structure and exchanged for endogenous CaM on myosin V at low stoichiometry (on average $<$0.5 labelled CaM light chains per double-headed myosin V molecule). Labelled myosin V molecules in a sample chamber on a fused silica microscope slide diffused from the bulk medium to interact with biotin- and AEDANS-labelled F-actin, which was immobilized on the slide surface (see Methods). Total internal reflection fluorescence microscopy[18,19] was used to image alternately the AEDANS–actin and rhodamine-labelled myosin V at the slide surface with evanescent waves at two distinct wavelengths. Individual rhodamine-labelled myosin V molecules, which were localized with an actin filament and moved along it when ATP was present, were selected for further investigation. These molecules were excited by an evanescent wave with four different polarization states switched (time-multiplexed) at intervals of 5 or 10 ms each, in aggregate filling out the three orthogonal spatial directions of optical polarization (x and y in the plane of the microscope slide, and z along the microscope optical axis; see Methods). The fluorescence was resolved into its components linearly polarized along the x and y axes, and was detected by two photon-counting avalanche photodiodes. The four time-multiplexed excitation and two simultaneously detected emission polarizations resulted in eight polarized fluorescence intensities for each successive 20- or 40-ms time point.

Fluorescence traces from rhodamine-labelled myosin V molecules containing single fluorophores were identified by a characteristic

intensity as well as simultaneous discrete photobleaching of all polarized intensities to background levels (Figs 1 and 2). Data were obtained from myosin V molecules interacting with actin filaments at 0 and 5 μM ATP with 40-ms time resolution, and at 40 μM ATP with 20-ms time resolution. Many of the molecules at 5 μM ATP (Fig. 1) and at 40 μM ATP (Supplementary Information) exhibited polarized fluorescence intensity levels that repeatedly underwent transitions back and forth in opposite directions. In Fig. 1, these transitions are most apparent in the intensities labelled ${}_{s1}I_y$ and ${}_{s2}I_x$ (see Methods for definitions). A weighted sum of all eight intensities (I_{Tot}), representing the total fluorescence independent of orientation, was constant, indicating that the intensity changes of the individual traces were due to abrupt rotations of the fluorophore. As the dual covalent linkage between the fluorophore and CaM fixes their relative orientation, these results imply that the LCD of myosin V tilts back and forth. For each time point in the single-molecule trace, the polarized intensities were fit to a set of equations to determine the total intensity (I_{Fit}), the axial angle (β) of the fluorophore relative to the actin axis, the azimuthal angle (α) around that axis, and the half-angle (δ) of a cone describing the wobbling motion of the fluorophore[20] on a timescale much slower than 4 ns but much faster than 10 ms (Fig. 1, lower panels and inset). The abrupt jumps of fluorescence intensity are caused by large changes in the β-value between periods of relatively steady β, as predicted by the hand-over-hand model.

To clarify the time course of these tilting motions relative to the noise in the recordings, individual transitions from many molecules were effectively synchronized by shifting their time bases to align the start times, and then averaged. The average angular traces derived from this procedure (Fig. 3; see also Supplementary Information) show that β-values changed by 40–50° and that this change was abrupt relative to the 20–40-ms recording time resolution. Furthermore, the averaging procedure revealed a step change of 15–20° in α. Whether this angle change implies left- or right-handed pitch in the step is not discernable from the current data owing to symmetries of the probe dipole and the experimental setup. The mobility parameter, δ, averaged 30–35° and changed much less than α or β. A small spike in δ at the transition is probably a sampling artefact due to limited temporal resolution and time-multiplexing of the excitation polarizations. These results imply that, at the ATP concentrations studied, any intermediate state with a different LCD orientation, such as that associated with a detached head, can occupy at most 10% of the average cycle time. This result is in agreement with a hand-over-hand model in which both heads of myosin V are attached to actin for most of the ATPase cycle.

Traces from a subset of molecules observed with 5 or 40 μM ATP, and nearly all traces recorded at 0 ATP (with apyrase present, Fig. 2), showed constant intensities, corresponding to steady angles. Angular transitions were observed at 0 ATP only rarely (0.1 events per molecule as compared with 3.1 and 2.4 for 5 and 40 μM ATP, respectively), consistent with occasional photochemical processes, the details of which will be reported elsewhere (M.E.Q., J.N.F. and Y.E.G., manuscript in preparation). None of the traces at 0 ATP showed the reversible and repeated transitions observed at 5 and 40 μM ATP, indicating that the orientation of a myosin V molecule bound to actin was stable in the absence of ATP.

Angular distributions

To characterize further the LCD orientations, an average β-value was calculated over each interval of the traces where the β-value was steady. This procedure resulted in many average β-values for each molecule that exhibited tilting at 5 and 40 μM ATP, but only one (or occasionally two) average β-value for each molecule that did not exhibit tilting at 0, 5 and 40 μM ATP. Distributions of average β-values for these groups of molecules showed discrete peaks that were fitted by gaussian-shaped curves (Fig. 4, Table 1 and Supplementary Information). An angular component with peak β at 27–30° and a relatively small wobble amplitude (δ_1 = 32–36°) was detected for molecules in the absence of ATP and for molecules exhibiting tilting at 5 and 40 μM ATP. Dispersion of these angular

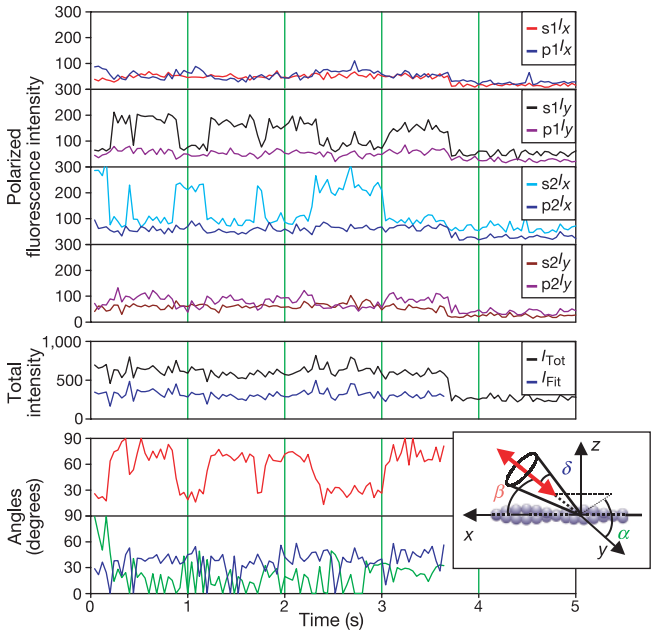

Figure 1 Data trace from a single myosin V molecule translocating along actin in the presence of 5 μM ATP. Polarized fluorescence intensities have units of photocounts per 10-ms gate; total intensities have units of photocounts per 40-ms cycle. Polarized intensity subscripts indicate excitation/detection polarizations as defined in the Methods. I_{Fit} is the total intensity determined by fitting the polarized fluorescence intensities; I_{Tot} is calculated from the polarized intensities as described in the Methods and should approximate I_{Fit} plus background. The single discrete decrease of all intensities to background levels at 3.7 s is due to photobleaching of the fluorophore. The inset defines β, α and δ (red, green and blue traces, respectively, in bottom panels) relative to the actin filament and the microscope frame, which is defined with the stage in the *x*–*y* plane.

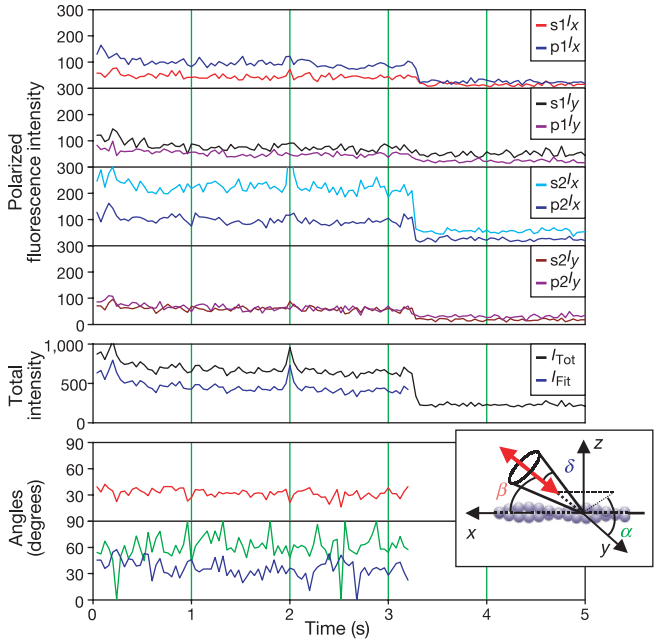

Figure 2 Data trace from a myosin V molecule bound to actin in the absence of ATP. All traces are relatively flat except for noise until the probe bleaches at 3.3 s.

components, $\sigma_{\beta 1}$ (Table 1), was lower at 0 ATP, reflecting the well-defined orientation of an attached myosin head near the end of its working stroke in the absence of ATP. Thus, it is likely that this angular component (at $\bar{\beta}_1 = 27$–$30°$) also represents the end of the working stroke in the active case. In the hand-over-hand mechanism, this corresponds to the trailing head with its LCD tilted forward towards the barbed end of the actin filament.

An angular component with a higher β-value, peaking at 72–78° for the tilting molecules at 5 and 40 μM ATP, would then represent the leading heads. Owing to symmetries of the probe dipole and the experimental setup, it is possible that the two β-peaks are actually on opposite sides of the plane perpendicular to actin (that is, one peak is at $180° - \beta$). As discussed later, the peak at $\bar{\beta}_2 = 72$–$78°$ for the tilting molecules probably represents probes at 108–102°.

For the set of molecules that did not tilt in the presence of ATP, the average β-distributions peaked at 52–54° and the mobility ($\bar{\delta}_2$) was 42–45° (Fig. 4b, Table 1 and Supplementary Information). These values match a component in the 0 ATP distribution with similar β- and δ-values, suggesting that both correspond to the same population of labelled CaM light chains. The absence of tilting may indicate that these CaM light chains are bound to a different site on myosin V than those that display tilting. If a labelled CaM were bound to a myosin V molecule outside the LCD, it would not be expected to tilt. Another potential explanation for non-tilting CaM light chains is that the LCD of the leading head may bend after attaching to actin, so that the section of LCD closest to the motor domain retains the same orientation in both leading and trailing positions. In that case, a CaM bound to this proximal region of the LCD would not exhibit tilting. It is also possible that non-tilting traces represent CaM light chains associated with myosin V heads that have stopped moving. Such heads could be detached from actin, but remain close to the surface if, for instance, their partner heads were still bound to actin. For molecules in the absence of ATP, double-headed attachments are unlikely[13], so the two components in Fig. 4c may represent attached ($\bar{\beta}_1 = 27°$, $\bar{\delta}_1 = 36°$) and detached ($\bar{\beta}_2 = 51°$, $\bar{\delta}_2 = 46°$) heads.

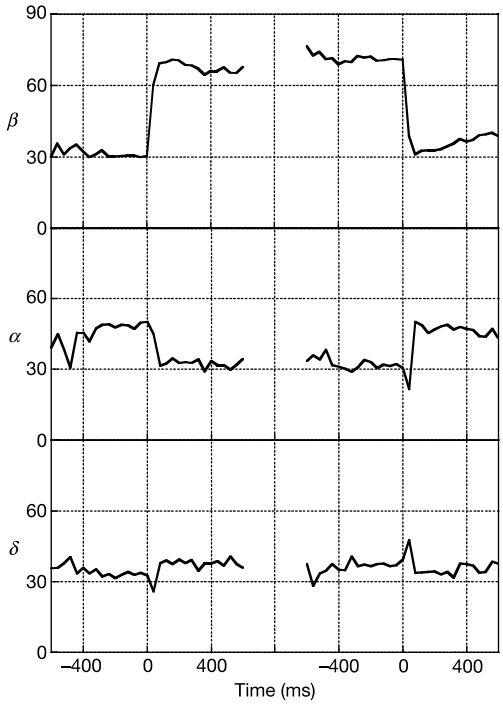

Figure 3 Transition averages. Point-by-point averages of 208 tilting events from 86 molecules in the presence of 5 μM ATP were determined after synchronizing the transitions at the points where the β-value abruptly increased or decreased. The time course shows that the tilting is rapid and incorporates axial (β) and azimuthal (α) components.

Kinetics of tilting and translocation

For each molecule that exhibited tilting, structural events containing an interval of steady β flanked by discrete transitions were divided into two groups with average β-values either greater or less than 50°. Event dwell times were measured as the interval between the beginnings of consecutive events. Histograms of these dwell times showed approximately exponential decay with no significant difference in rate between events at high and low β-values (see Methods).

Histograms of aggregate dwell time including both high and low β-events are shown in Fig. 5. The event durations decreased markedly when the ATP concentration was raised from 5 to 40 μM. The rate constant for a single exponential decay fitted to each of these histograms (dashed lines) increased 2.7-fold for the 8-fold increase in ATP concentration (see Methods), indicating that the dwell times are determined by both an ATP-dependent kinetic process and an ATP-independent process. Therefore, a double exponential curve assuming two sequential processes, one with rate $k_1 \cdot [\mathrm{ATP}]$, and the other with rate k_2, independent of [ATP], was fitted to the data in both histograms (solid lines in Fig. 5a, b). This global analysis yielded rate constants of $k_1 = 1.1 \pm 0.2 \times 10^6\,\mathrm{M^{-1}\,s^{-1}}$, and $k_2 = 12.0 \pm 1.7\,\mathrm{s^{-1}}$ (95% confidence limits). These values are in good agreement with the ATP-binding rate of $0.9 \times 10^6\,\mathrm{M^{-1}\,s^{-1}}$ and the ADP release rate of 12–16 $\mathrm{s^{-1}}$ measured biochemically[8], and with the two rate constants ($0.9 \times 10^6\,\mathrm{M^{-1}\,s^{-1}}$

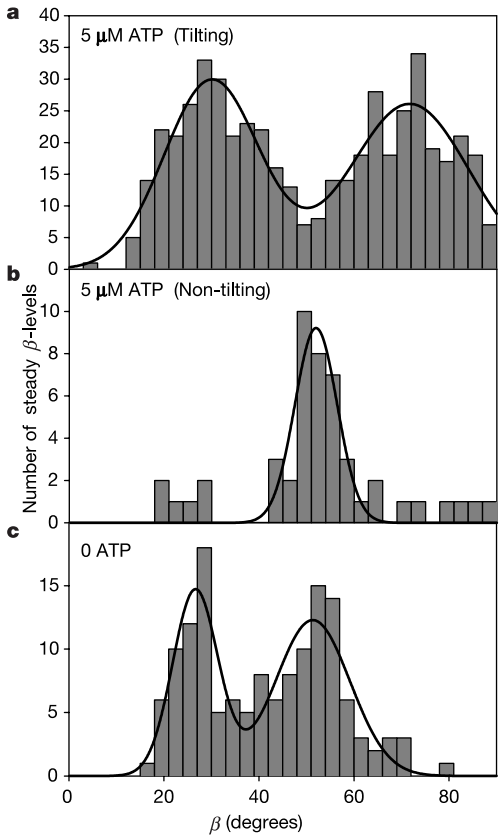

Figure 4 Distributions of average β-values in the presence and absence of ATP. **a**, Myosin V molecules translocating and showing repeated tilting events at 5 μM ATP. **b**, Molecules translocating in the presence of 5 μM ATP but not showing angle changes. **c**, Myosin V co-localized with actin filaments in the absence of ATP. Solid lines indicate the best fits to single or double gaussian-shaped profiles. Parameters of the fits are given in Table 1.

Table 1 **Peak angles, dispersions and mobilities**

ATP concentration	*n*	Fraction in first peak	$\bar{\beta}_1$	$\sigma_{\beta 1}$	$\bar{\delta}_1$	$\sigma_{\delta 1}$	$\bar{\beta}_2$	$\sigma_{\beta 2}$	$\bar{\delta}_2$	$\sigma_{\delta 2}$
5 μM tilting	86	0.48 ± 0.04	30.0 ± 0.9	10.0 ± 0.9	34.4	13.6	71.7 ± 1.1	12.4 ± 1.5	37.3	11.2
40 μM tilting	100	0.46 ± 0.03	27.1 ± 0.6	8.92 ± 0.6	31.6	11.4	77.8 ± 1.3	13.1 ± 1.5	30.4	12.1
5 μM non-tilting	48	–	–	–	–	–	52.0 ± 0.5	4.5 ± 0.5	44.9	9.0
40 μM non-tilting	101	–	–	–	–	–	54.2 ± 0.7	6.2 ± 0.7	41.9	8.3
0 μM	140	0.42 ± 0.04	26.6 ± 0.6	4.78 ± 0.6	36.1	7.6	51.3 ± 0.9	7.8 ± 1.0	46.4	6.0

Fits of single or double gaussian profiles to the histograms in Fig. 4 (5 μM tilting/non-tilting and 0 ATP) and Supplementary Fig. 3 (40 μM tilting/non-tilting) gave values for the peak axial angle ($\bar{\beta}$) and standard deviation (σ_β) of each gaussian profile. Uncertainties in these fitted parameters (for example, ±0.9) are given as standard errors. δ-value (wobble amplitude as described in the main text), mean ($\bar{\delta}$) and standard deviation (σ_δ) were calculated for the population of steady β-levels in each gaussian profile (see Methods). Angles are given in degrees. *n* is the number of molecules. The number of steady β-levels in the 5-μM-ATP tilting and 40-μM-ATP tilting populations were 495 and 576, respectively.

and 13 s^{-1}) that describe single-molecule mechanical stepping rates determined by optical trapping experiments[11]. Therefore, sequential tilts of the myosin V LCD each correspond to the binding of one ATP molecule, release of one ADP molecule, and a single mechanical step, which are all consistent with the hand-over-hand model.

Average translocation velocities (V) were measured in the same experiments and were fitted by the hyperbolic relation $V = V_{max}[ATP]/([ATP] + K_M)$ (Fig. 5c), yielding $V_{max} = 453 \pm 10$ nm s^{-1} and $K_M = 11.7 \pm 1.2$ μM (95% confidence limits). Within uncertainties, K_M is equal to the ratio of k_2 to k_1, implying that the same processes control the rate of the observed structural changes and the mechanical displacements. To further quantify this relationship, the product of the velocity measured at each ATP concentration and the corresponding mean event duration, $\tau_e = \left(\frac{1}{k_1[ATP]} + \frac{1}{k_2}\right)$, was calculated to determine the average distance a myosin V molecule moves per discrete rotation of the LCD. $V \cdot \tau_e$ values at 5 and 40 μM ATP were 36.2 ± 4.0 and 37.4 ± 3.5 nm (95% confidence limits), respectively, similar to the crossover distance of actin's long-pitch helix. These values provide an estimate of the stride length of the myosin V molecule solely from its structural dynamics and independent of other mechanical or biochemical data. This stride length per structural change is comparable to the unitary mechanical displacements previously measured[11], confirming the conclusion above that the LCD tilts once per mechanical step.

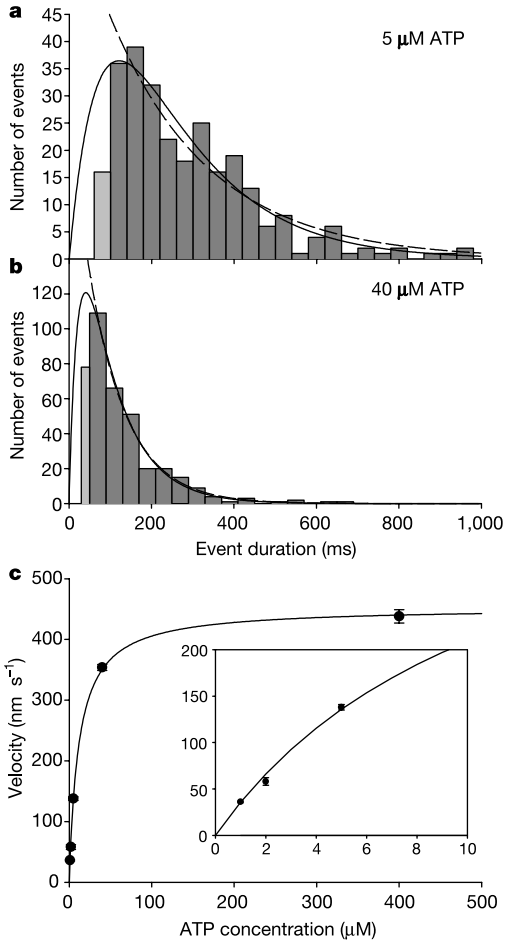

Figure 5 Event kinetics. **a**, **b**, Distributions of event dwell times determined from β-traces at 5 μM (**a**) and 40 μM (**b**) ATP (Fig. 1 and Supplementary Information). Dashed curves are single exponential fits; solid curves represent the global fit of a two-step model explained in the text. The first bins (light-grey bars) in **a** and **b** are under-populated owing to limited time resolution and were ignored during fitting. In **b**, the height of this bin was doubled because its width is halved. **c**, Average translocation velocities versus ATP concentration (inset shows an expanded view). Error bars indicate standard errors of the mean.

Discussion

Our study represents the first direct time-resolved measurement of tilting in an actively translocating motor protein sufficient to explain the observed mechanical step. The head–tail junction of a myosin V molecule travels 36–37 nm for each major tilting motion, as shown above. Consider the lever arm provisionally to be a rigid 24-nm rod. The axis of the lever tilts, for instance, from 40° to 140° when stepping from the trailing to the leading position ((cos 40°–cos 140°)24 nm = 36.8 nm). With these angles, the head–tail junctions of the two heavy chains meet at the same radial distance from actin (sin 40° = sin 140°). Our rhodamine probe, oriented 40° from the lever axis (see Supplementary Information), is observed to tilt from about 30° to about 105° (Fig. 4, peak plotted near 75° = 180° − 105°). The slightly smaller magnitude of tilting can be accommodated if the probe dipole is not oriented in the plane of the lever arm rotation and the lever twists about its own axis by 10° or by 85° (calculation given in Supplementary Information). The probe data are compatible with other angles of lever tilt and twist if the CaM-binding region is flexible[13] or if the two head–tail junctions do not coincide. The data thus provide clear evidence for the lever arm function of the CaM-binding region of myosin V.

Single-molecule fluorescence polarization techniques have been used previously for studies of protein domain rotations[20]. Rotation of F_1-ATPase[21] and actin[22], and transitions between disordered and ordered states of myosin II[23] were detected during ATP-driven motility. Spontaneous motions of DNA[24] and kinesin[25] have been detected, the latter with a bifunctional probe similar to that used here. All of these previous studies were limited to detecting the two-dimensional projection of the probe orientation onto the plane of the microscope stage. With myosin V, determination of the lever arm rotations relative to actin required measurement of the three-dimensional probe orientation (that is, the probe angle relative to the microscope optical axis in addition to the orientation of the projection onto the stage). Other techniques have been described for measuring the three-dimensional orientations of single fluorophores[20]. However, these have not yet been used for biomolecular structural dynamics and are currently limited by specialized sample requirements[26,27] or low time resolution[28,29]. Robust, time-resolved measurement of three-dimensional probe orientation is a major advantage of the technique described here. Similar three-

dimensional angular data should be relevant to many other biological systems that can operate near a surface.

A model of myosin V processivity must explain the following structural observations obtained in the present study: (1) in the presence of ATP, the LCD tilts between two discrete axial angles that differ by ≥45° or ≥75°; (2) the two states corresponding to these orientations have approximately the same amplitude of 4 ns to 10 ms mobility; (3) the duration of occupancy in the two orientations is the same, within the 20–40-ms time resolution of the current experiments; (4) no additional structural states with distinct LCD orientations or mobilities are occupied for more than 20–40 ms; (5) myosin V translocates about 37 nm on average for each LCD rotation; and (6) the rates of the observed structural changes, combined with earlier measurements, imply one rotation per unitary mechanical step, and per hydrolysis of an ATP molecule.

These results imply that the approximately 37-nm mechanical steps of myosin V involve transitions of the individual heads between two structural states, both bound to actin strongly enough to limit the mobility of the CaM-binding region. These two states are probably a leading head at the beginning of its working stroke and a trailing head at the end. Several models other than the hand-over-hand mechanism have been proposed to explain processive translocation of motor proteins along cytoskeletal tracks—in particular, 'biased diffusion', 'inchworm' and 'hotspot' models[30–35]. Biased diffusion and hotspot models, as well as some hand-over-hand models[36] postulate that, for a significant portion of a catalytic cycle, only one head of the motor protein is strongly bound to its track. They typically do not include high occupancy of the state with two heads firmly attached to actin that predominates in the present experiments. In the typical inchworm model[33], the structural state of neither head changes on completion of consecutive steps, which is incompatible with our observation that individual heads oscillate between two distinct orientations. Of the proposed models for myosin V processivity, the hand-over-hand model, including a working stroke generated by a tilting lever arm, most readily explains the observations reported here.

Note added in proof: Burgess *et al.*[44] have recently published results that are difficult to reconcile with one of our possible explanations for the non-tilting CaM light chains in the presence of ATP: the bent neck model. □

Methods

Protein preparation

Rabbit muscle actin was purified[37] and labelled[38] at Cys 374 with 1,5-IAEDANS. F-actin, at 1 μM total monomer concentration, 14% unlabelled, 81% AEDANS-labelled, and 5% biotin-labelled (Cytoskeleton), was stabilized with 2.6 μM phalloidin (Molecular Probes). Residues Pro 66 and Ala 73 of chicken CaM[39] were mutated to Cys (QuikChange, Stratagene; plasmid supplied by H. L. Sweeney). Mutant CaM was expressed[40], labelled[17] and purified (Supplementary Information). Electrospray mass spectrometry, after endoproteinase Asp-N (Roche Diagnostics) digestion, confirmed rhodamine cross-linking of Cys 66 and Cys 73. Chick brain myosin V was purified[41] and labelled by exchanging[12] endogenous CaM with a 1:10 mixture of bifunctional rhodamine-labelled calmodulin and wild-type CaM.

Motility assay

Fused silica slides (Quartz Scientific), spin-coated with 2 mg ml^{-1} poly(methyl methacrylate) (Aldrich Chemical, no. 37,003-7) in methylene chloride, were incorporated into approximately 10-μl sample chambers with glass coverslips and double-sided adhesive tape. F-actin was bound to the poly(methyl methacrylate) surface through biotinylated BSA and streptavidin[12]. Flow aligned the F-actin with the microscope x axis. Myosin V labelled with bifunctional rhodamine-labelled calmodulin was introduced into the sample chamber at about 10–1,000 pM in 25 mM KCl, 2 mM $MgCl_2$, 1 mM EGTA, 100 μg ml^{-1} wild-type CaM, 100 mM dithiothreitol, 20 mM HEPES, pH 7.6, and ATP as indicated. Compatible with earlier work[8], k_1 and K_M were calculated based on total ATP concentration. With the dissociation constant (K_d) for Mg^{2+} binding to ATP of 133 μM, MgATP concentration would be 6% less[42]. This correction does not affect calculated step sizes. For 0 ATP experiments, the buffer included 2 U ml^{-1} apyrase (Sigma).

Single-molecule fluorescence polarization

Full details of this technique will be described elsewhere (J.N.F., M.E.Q. and Y.E.G., manuscript in preparation). Briefly, a 1 mW, 355-nm laser (JDS Uniphase) and a 10–20 mW, 532-nm laser (Lightwave Electronics) were directed towards the sample chamber through a BK7 prism (ESCO Products) and index-matching liquid (Cargille Laboratories) at a glancing angle relative to the microscope slide. Total internal reflection generated evanescent waves near the sample chamber surface[18,19]. The 532-nm laser direction and polarization were modulated by Pockels cells (Conoptics) at 5 or 10 ms, producing four excitation polarizations. s1 and s2 generated linear polarizations along y and x axes; p1 and p2 produced polarizations approximately along the z axis with small components along x and y, respectively[20]. Camera (V/ICCD, Roper Scientific) images were used to identify actin filament location and orientation, and individual rhodamines. A piezo-electric stage (Polytec PI) centred a single labelled myosin V molecule co-localized with actin on the microscope stage. A ×100 1.2 NA water immersion objective projected fluorescence through a polarizing beam splitter to resolve x and y polarizations onto two avalanche photodiodes (Perkin Elmer, SPCM-AQR-16). Total fluorescence was calculated using $I_{Tot} = ({}_{s1}I_x + {}_{s1}I_y + {}_{s2}I_x + {}_{s2}I_y) + 0.885({}_{p1}I_x + {}_{p1}I_y + {}_{p2}I_x + {}_{p2}I_y)$, which is approximately independent of probe orientation.

Data analysis

Single molecules were identified by total intensity and single-step photobleaching. In traces with two bleaching steps, only data after the first step were analysed. Analytical equations (to be described elsewhere: J.N.F, M.E.Q. and Y.E.G., manuscript in preparation) were fitted to data for each time point to obtain I_{Fit}, β, α and δ. Transitions where the β-value changed abruptly from one approximately constant value to another were identified manually using defined criteria. For averaging, transitions were grouped according to whether the β-value increased or decreased. Each transition was shifted to set the preceding datum to 0 ms and traces were averaged between the preceding and following adjacent transitions.

Histograms of β-values

β-values were averaged for each region of a trace where β remained approximately constant (steady β-level), except the last region in traces exhibiting tilting. Three-degree bin width histograms of averages were fitted by gaussian distributions, $\rho(\beta)$, given by:

$$\rho(\beta) = A\left(\frac{f}{\sigma_{\beta 1}\sqrt{2\pi}}\right)\exp\left[-\frac{1}{2}\left(\frac{\beta-\bar{\beta}_1}{\sigma_{\beta 1}}\right)^2\right] + A\left(\frac{1-f}{\sigma_{\beta 2}\sqrt{2\pi}}\right)\exp\left[-\frac{1}{2}\left(\frac{\beta-\bar{\beta}_2}{\sigma_{\beta 2}}\right)^2\right]$$

where A is the product of the total number of steady β-levels and the bin width; f is the fraction of steady β-levels in the first gaussian peak. For 5 and 40 μM ATP data exhibiting tilting, mean ± s.d. of δ-values were determined for the two groups of steady β-intervals with average β greater or less than 50°. For 0 ATP data, the groups were split at 39°. For 5 and 40 μM ATP data without tilting, they were determined for average β within $\bar{\beta}_2 \pm 3\sigma_{\beta 2}$.

Event dwell times

Dwell times were differences between the starting times of consecutive events with β-values on opposite sides of 50°. Separating events into populations with β-values greater or less than 50° gave single exponential fits to histograms of 5 μM ATP dwell times, with rate constants of 4.2 ± 0.3 s^{-1} and 4.1 ± 0.3 s^{-1} (±standard error), respectively. The corresponding rates for the 40 μM ATP data were 10.1 ± 0.4 s^{-1} and 11.7 ± 0.7 s^{-1}. A single exponential fit to histograms with all event data (without discriminating by β-value) gave rate constants of 4.1 ± 0.2 s^{-1} for 5 μM ATP and 10.9 ± 0.4 s^{-1} for 40 μM ATP.

The 5 and 40 μM ATP histograms were also fit simultaneously to:

$$\rho(t) = A\left(\frac{k_1[\mathrm{ATP}]k_2}{k_1[\mathrm{ATP}]-k_2}\right)(\exp(-k_2 t) - \exp(-k_1[\mathrm{ATP}]t))$$

where t is dwell time and A is amplitude (different for the two ATP concentrations). This fit used bin widths equal to the measurement time resolutions (MTR): 40 ms for 5 μM ATP and 20 ms for 40 μM ATP. Because selection criteria required events to contain ≥2 time points, no dwell times equal to the MTR were scored. Bins at twice the MTR also had fewer events than expected from the fitted curves, presumably being undercounted owing to noise. These bins (light-grey bars in Fig. 5) were therefore ignored. Monte-Carlo simulations determined 95% confidence limits for fitted rates[43].

Velocity measurements

Velocities of individual myosin V molecules were determined from images with 10-ms-resolution time stamps taken at approximately 1-s intervals.

Received 16 December 2002; accepted 3 March 2003; doi:10.1038/nature01529.

1. Reedy, M. K., Holmes, K. C. & Tregear, R. T. Induced changes in orientation of the cross-bridges of glycerinated insect flight muscle. *Nature* **207,** 1276–1280 (1965).
2. Rayment, I. *et al.* Structure of the actin–myosin complex and its implications for muscle contraction. *Science* **261,** 58–65 (1993).
3. Spudich, J. A. The myosin swinging cross-bridge model. *Nature Rev. Mol. Cell Biol.* **2,** 387–392 (2001).
4. Geeves, M. A. & Holmes, K. C. Structural mechanism of muscle contraction. *Annu. Rev. Biochem.* **68,** 687–728 (1999).
5. Irving, M. & Piazzesi, G. Motions of myosin heads that drive muscle contraction. *News Physiol. Sci.* **12,** 249–254 (1997).
6. Goldman, Y. E. Wag the tail: Structural dynamics of actomyosin. *Cell* **93,** 1–4 (1998).
7. Cheney, R. E. *et al.* Brain myosin-V is a two-headed unconventional myosin with motor activity. *Cell* **75,** 13–23 (1993).
8. De La Cruz, E. M., Wells, A. L., Rosenfeld, S. S., Ostap, E. M. & Sweeney, H. L. The kinetic mechanism of myosin V. *Proc. Natl Acad. Sci. USA* **96,** 13726–13731 (1999).
9. Mehta, A. D. *et al.* Myosin-V is a processive actin-based motor. *Nature* **400,** 590–593 (1999).
10. Mehta, A. Myosin learns to walk. *J. Cell Sci.* **114,** 1981–1998 (2001).
11. Rief, M. *et al.* Myosin-V stepping kinetics: A molecular model for processivity. *Proc. Natl Acad. Sci. USA* **97,** 9482–9486 (2000).

12. Sakamoto, T., Amitani, I., Yokota, E. & Ando, T. Direct observation of processive movement by individual myosin V molecules. *Biochem. Biophys. Res. Commun.* **272,** 586–590 (2000).
13. Walker, M. L. *et al.* Two-headed binding of a processive myosin to F-actin. *Nature* **405,** 804–807 (2000).
14. Veigel, C., Wang, F., Bartoo, M. L., Sellers, J. R. & Molloy, J. E. The gated gait of the processive molecular motor, myosin V. *Nature Cell Biol.* **4,** 59–65 (2002).
15. Moore, J. R., Krementsova, E. B., Trybus, K. M. & Warshaw, D. M. Myosin V exhibits a high duty cycle and large unitary displacement. *J. Cell Biol.* **155,** 625–635 (2001).
16. Corrie, J. E. T. *et al.* Dynamic measurement of myosin light-chain-domain tilt and twist in muscle contraction. *Nature* **400,** 425–430 (1999).
17. Corrie, J. E. T., Craik, J. S. & Munasinghe, V. R. N. A homobifunctional rhodamine for labeling proteins with defined orientations of a fluorophore. *Bioconjug. Chem.* **9,** 160–167 (1998).
18. Axelrod, D., Burghardt, T. P. & Thompson, N. L. Total internal reflection fluorescence. *Annu. Rev. Biophys. Bioeng.* **13,** 247–268 (1984).
19. Funatsu, T., Harada, Y., Tokunaga, M., Saito, K. & Yanagida, T. Imaging of single fluorescent molecules and individual ATP turnovers by single myosin molecules in aqueous solution. *Nature* **374,** 555–559 (1995).
20. Forkey, J. N., Quinlan, M. E. & Goldman, Y. E. Protein structural dynamics by single-molecule fluorescence polarization. *Prog. Biophys. Mol. Biol.* **74,** 1–35 (2000).
21. Adachi, K. *et al.* Stepping rotation of F_1-ATPase visualized through angle-resolved single-fluorophore imaging. *Proc. Natl Acad. Sci. USA* **97,** 7243–7247 (2000).
22. Sase, I., Miyata, H., Ishiwata, S. & Kinosita, K. Jr Axial rotation of sliding actin filaments revealed by single-fluorophore imaging. *Proc. Natl Acad. Sci. USA* **94,** 5646–5650 (1997).
23. Warshaw, D. M. *et al.* Myosin conformational states determined by single fluorophore polarization. *Proc. Natl Acad. Sci. USA* **95,** 8034–8039 (1998).
24. Ha, T., Glass, J., Enderle, Th., Chemla, D. S. & Weiss, S. Hindered rotational diffusion and rotational jumps of single molecules. *Phys. Rev. Lett.* **80,** 2093–2096 (1998).
25. Sosa, H., Peterman, E. J. G., Moerner, W. E. & Goldstein, L. S. B. ADP-induced rocking of the kinesin motor domain revealed by single-molecule fluorescence polarization microscopy. *Nature Struct. Biol.* **8,** 540–544 (2001).
26. Bopp, M. A., Jia, Y., Li, L., Cogdell, R. J. & Hochstrasser, R. M. Fluorescence and photobleaching dynamics of single light-harvesting complexes. *Proc. Natl Acad. Sci. USA* **94,** 10630–10635 (1997).
27. Empedocles, S. A., Neuhauser, R. & Bawendi, M. G. Three-dimensional orientation measurements of symmetric single chromophores using polarization microscopy. *Nature* **399,** 126–130 (1999).
28. Betzig, E. & Chichester, R. J. Single molecules observed by near-field scanning optical microscopy. *Science* **262,** 1422–1425 (1993).
29. Dickson, R. M., Norris, D. J. & Moerner, W. E. Simultaneous imaging of individual molecules aligned both parallel and perpendicular to the optic axis. *Phys. Rev. Lett.* **81,** 5322–5325 (1998).
30. Vale, R. D. & Oosawa, F. Protein motors and Maxwell's demons: Does mechanochemical transduction involve a thermal ratchet? *Adv. Biophys.* **26,** 97–134 (1990).
31. Block, S. M. Kinesin: What gives? *Cell* **93,** 5–8 (1998).
32. Okada, Y. & Hirokawa, N. A processive single-headed motor: Kinesin superfamily protein KIF1A. *Science* **283,** 1152–1157 (1999).
33. Hua, W., Chung, J. & Gelles, J. Distinguishing inchworm and hand-over-hand processive kinesin movement by neck rotation measurements. *Science* **295,** 844–848 (2002).
34. Tanaka, H. *et al.* The motor domain determines the large step of myosin-V. *Nature* **415,** 192–195 (2002).
35. Nishikawa, S. *et al.* Class VI myosin moves processively along actin filaments backward with large steps. *Biochem. Biophys. Res. Commun.* **290,** 311–317 (2002).
36. De La Cruz, E. M., Ostap, E. M. & Sweeney, H. L. Kinetic mechanism and regulation of myosin VI. *J. Biol. Chem.* **276,** 32373–32381 (2001).
37. Pardee, J. D. & Spudich, J. A. Purification of muscle actin. *Methods Cell Biol.* **24,** 271–289 (1982).
38. Cooper, J. A., Walker, S. B. & Pollard, T. D. Pyrene actin: Documentation of the validity of a sensitive assay for actin polymerization. *J. Muscle Res. Cell Motil.* **4,** 253–262 (1983).
39. Putkey, J. A. *et al.* Chicken calmodulin genes. *J. Biol. Chem.* **258,** 11864–11870 (1983).
40. Putkey, J. A., Slaughter, G. R. & Means, A. R. Bacterial expression and characterization of proteins derived from the chicken calmodulin cDNA and a calmodulin processed gene. *J. Biol. Chem.* **260,** 4704–4712 (1985).
41. Cheney, R. E. Purification and assay of myosin V. *Methods Enzymol.* **298,** 3–18 (1998).
42. Moisescu, D. G. & Thieleczek, R. Sarcomere length effects on the Sr^{2+}- and Ca^{2+}-activation curves in skinned frog muscle fibres. *Biochim. Biophys. Acta* **546,** 64–76 (1979).
43. Press, W. H., Teukolsky, S. A., Vetterling, W. T. & Flannery, B. P. *Numerical Recipes in C: The Art of Scientific Computing* 2nd edn (Cambridge Univ. Press, Cambridge, UK, 1992).
44. Burgess, S. *et al.* The prepower stroke conformation of myosin V. *J. Cell. Biol.* **159,** 983–991 (2002).

Supplementary Information accompanies the paper on *Nature*'s website (**http://www.nature.com/nature**).

Acknowledgements This work was supported by the NIH and Medical Research Council. We thank H. Shuman, M. Ostap, H. Higuchi, M. Mooseker, R. Cheney, A. Houdusse, D. Trentham, R. Ferguson, B. Brandmeier and F. Vanzi for discussions, and R. Munasinghe, I. Gertsman, S. Manz, D. Keleti and N. Tang for technical assistance.

Competing interests statement The authors declare that they have no competing financial interests.

Correspondence and requests for materials should be addressed to Y.E.G. (e-mail: goldmany@mail.med.upenn.edu).